Imaging Probes Hot Paper

Deutsche Ausgabe: DOI: 10.1002/ange.201504441
Internationale Ausgabe: DOI: 10.1002/anie.201504441

A Small-Molecule Probe for Selective Profiling and Imaging of Monoamine Oxidase B Activities in Models of Parkinson's Disease

*Lin Li, Cheng-Wu Zhang, Jingyan Ge, Linghui Qian, Bing-Han Chai, Qing Zhu, Jun-Seok Lee, Kah-Leong Lim, and Shao Q. Yao**

Abstract: *The design of the first dual-purpose activity-based probe of monoamine oxidase B (MAO-B) is reported. This probe is highly selective towards MAO-B, even at high MAO-A expression levels, and could sensitively report endogenous MAO-B activities by both in situ proteome profiling and live-cell bioimaging. With a built-in imaging module as part of the probe design, the probe was able to accomplish what all previously reported MAO-B imaging probes failed to do thus far: the live-cell imaging of MAO-B activities without encountering diffusion problems.*

MAO-A and MAO-B are two isoforms of the monoamine oxidases that are localized predominantly in the mitochondrial outer membrane and catalyze the deamination of important neurotransmitters.[1] Although these two flavoenzymes have a sequence identity of 70%, they have distinct physiological properties, substrate preferences, and inhibitor sensitivities.[2] Their over-activation is known to cause the excessive production of neurotoxic byproducts (e.g., H_2O_2) and promote neuronal dysfunctions, potentially leading to psychiatric disorders and neurodegenerative diseases.[3] Parkinson's disease (PD), for example, a common illness among older people, is often associated with significantly higher levels of MAO-B, but not MAO-A, activity in the brain.[2,4] Such elevated MAO-B activities cause the highly membrane-permeable H_2O_2 generated to readily diffuse from astrocytes to neighboring neuronal cells, leading to oxidative stress and eventual degeneration. Selegiline (**SE**, IC_{50} MAO-A/B = 250) and rasagiline (**RA**, IC_{50} MAO-A/B = 50.7) are two FDA-approved drugs for the treatment of early-stage PD (Figure 1); they work by selectively inhibiting the over-expressed MAO-B in patients.[5] To better understand the critical role of MAO-B in PD and its therapeutic implications, chemical methods that are capable of the sensitive detection of endogenous MAO-B activities and the accurate interrogation of MAO-B/drug interactions under native biological settings (e.g., live cells, tissues, or animals) have been developed.[6–10] Among them, fluorescence-based cell-imaging strategies are highly useful owing to their practicality, high sensitivity, and, in some cases, the capability of directly detecting MAO activities in deep tissues.[6–8] Such methods, however, suffer from one major drawback common to all small-molecule-based enzyme-detecting imaging probes, that is, the highly fluorescent reaction product of the probe may diffuse away from the enzyme active site, and is thus of limited utility in high-resolution studies of enzyme localization. Another key drawback is the lack of isoform-specific probes, even though this issue has recently been alleviated with the report of a spin-labeled probe[10] as well as a two-photon small-molecule probe (**U1** in Figure 1), which were employed for the highly specific and sensitive real-time imaging of MAO-B activities in various biological samples.[8] Recently, activity-based probes for the in situ profiling of MAO activities from complex mammalian proteomes have been reported for the first time.[9] Inspired by the development of activity-based protein profiling (ABPP),[11] Sieber, Breinbauer, and co-workers showed that **P3** (Figure 1), which was designed based on the known irreversible MAO inhibitor deprenyl, was able to covalently bind to MAO-A and MAO-B exclusively, thus providing novel opportunities for the chemoproteomic profiling of MAO activities in cells and tissues.[9] Notwithstanding, **P3** offers little MAO-A/B selectivity, especially under in vitro conditions or when the endogenous MAO expression levels are high. Like most other activity-based probes, **P3**, despite its good cell permeability, is ill-suited for the direct imaging of MAO activities in live cells and tissues owing to the lack of an internally built-in fluorophore. The terminal alkyne moiety in **P3** could in principle be used as a "click" handle for the two-step imaging of endogenous MAO activities, but chemical fixation of cells is normally required.[12] We envisioned that dual-purpose small-molecule probes[13] that are capable of both live-cell/tissue imaging and in situ profiling of endogenous MAO activities in an isoform-selective manner would be highly desirable. By combining

[*] Dr. L. Li,[+] Dr. J. Ge,[+] L. Qian, Prof. Dr. S. Q. Yao
Department of Chemistry, National University of Singapore
3 Science Drive 3, Singapore 117543 (Singapore)
E-mail: chmyaosq@nus.edu.sg
Dr. L. Li[+]
Key Laboratory of Flexible Electronics & Institute of Advanced Materials, National Jiangsu Synergistic Innovation Center for Advanced Materials, Nanjing Tech University
Nanjing, 211816 (P.R. China)
Dr. C.-W. Zhang,[+] B.-H. Chai, Prof. Dr. K.-L. Lim
National Neuroscience Institute
Singapore 308433 (Singapore)
Prof. Dr. Q. Zhu
Institute of Bioengineering
Zhejiang University of Technology
Hangzhou, 310014 (P.R. China)
Prof. Dr. J.-S. Lee
Molecular Recognition Research Center
Korea Institute of Science and Technology (KIST), and
Department of Biological Chemistry
University of Science & Technology (Republic of Korea)
[+] These authors contributed equally to this work.

Supporting information for this article is available on the WWW under http://dx.doi.org/10.1002/anie.201504441.

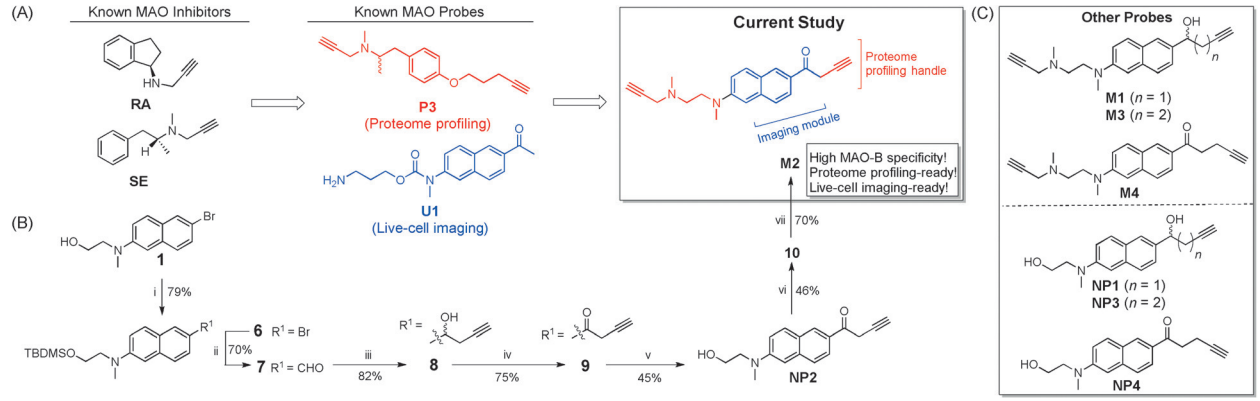

Figure 1. A) Molecular structures of known MAO inhibitors (rasagiline and selegiline), small-molecule probes (**P3** and **U1**), and the dual-purpose probe (**M2**) reported in the current study. B) Synthesis of **M2** (and its control probe **NP2**). Reaction conditions: i) *tert*-butyldimethylsilyl chloride, imidazole, 4-dimethylaminopyridine (cat.), CH_2Cl_2, 0 °C to RT, 24 h; ii) *n*BuLi, DMF, THF, −78 to −10 °C, 1.5 h; iii) 1-propynylmagnesium bromide, THF, −78 to −30 °C, 1.5 h; iv) MnO_2, acetone, 0 °C, 1 h; v) tetrabutylammonium fluoride, THF, 0 °C to RT, 2 h; vi) *N*-bromosuccinimide, PPh_3, CH_2Cl_2, 0 °C, 2 h; vii) methylpropargylamine, K_2CO_3, KI (cat.), CH_3CN, 100 °C (microwave), 45 min. C) Structures of other probes used in the current study.

information obtained from the sub-cellular localization and the large-scale cell/tissue-based proteome profiling of such probes, our understanding of how the up or down regulation of MAO-B affects the prognosis of PD patients could be significantly improved.

Herein, by combining key features of our previously reported MAO-B imaging probe **U1**[8] and the proteome-profiling-enabled probe **P3**,[9] we have successfully developed the first dual-purpose activity-based probe for MAO-B (**M2** in Figure 1). The subsequent evaluation of **M2** against a variety of biological samples, including recombinant MAO proteins, mammalian cell lysates, live mammalian cells, and mouse brain tissues, under both in situ chemoproteomic and live-cell imaging settings, indicated that **M2** was highly selective towards MAO-B even at high MAO-A expression levels, and could detect endogenous MAO-B activities with high sensitivities by both in-gel fluorescence scanning and microscopy techniques (Supporting Information, Figure S1). With a built-in imaging module (e.g., 2-methylamino-6-acetylnaphthalene or acedan) as part of the probe design, **M2** was able to accomplish what all existing MAO-B imaging probes failed to do thus far— the live-cell imaging of MAO-B activities without diffusion problems (Figure S1 A). This was made possible by its *N*-propargylamine group, which forms a stable covalent adduct upon reacting with MAO-B (Figure S1 B). To make **M2** ready for profiling, an additional terminal alkyne (i.e., the proteome profiling handle) was introduced at the carbonyl end of acedan. Upon in situ proteome labeling, the resulting probe-labeled proteins were readily detected by click chemistry with a suitable azide-containing reporter (e.g., Rh-biotin-N_3 in Figure S1 C), followed by SDS-PAGE/in-gel fluorescence scanning or affinity pull-down (PD)/Western blotting (WB) analysis.[11,14] We hypothesized that like for **U1**, the high MAO-B selectivity of **M2** could be achieved by retention of the acedan core moiety, which was essential for preferential binding to the relatively deep and shallow MAO-B active-site pocket.[8]

The synthesis of **M2**, together with control compound **NP2**, which lacks the essential *N*-propargylamine group, is shown in Figure 1 B. Several additional analogues, including **M4** (with one extra carbon atom at the terminal alkyne handle) and **M1**/**M3** (reduction of C=O in **M2**/**M4** to C–OH) as well as the corresponding control probes (**NP1**/**NP3**/**NP4**), were synthesized in a similar fashion (Figure 1 C and Schemes S1–S4). **M1** and **M3** were designed to probe the possible involvement of a hydrogen bond near the C=O group of **U1** in the MAO-B/**U1** binding complex.[8]

We first evaluated the photochemical, photophysical, and biochemical properties of these probes under physiological conditions (HEPES buffer with 0.02 % Triton X-100, pH 7.5; see Table S1 and Figure S2). All probes exhibited nearly identical fluorescence excitation and emission; for example, **M1**, **M2**, **M3**, and **M4** had absorption/emission maxima at 350/430 nm ($\varepsilon_{350} = 9900\,M^{-1}cm^{-1}$, $\Phi = 0.52$), 410/510 nm ($\varepsilon_{410} \approx 27\,600\,M^{-1}cm^{-1}$, $\Phi = 0.12$), 350/430 nm ($\varepsilon_{350} = 4100\,M^{-1}cm^{-1}$, $\Phi = 0.44$), and 380/510 nm ($\varepsilon_{380} = 32\,700\,M^{-1}cm^{-1}$, $\Phi = 0.15$), respectively. Obvious red-shifts were observed for the absorption/emission maxima of **M2** and **M4** when compared to **M1** and **M3**, which are likely due to the enhanced electron-withdrawing effect of C=O in acedan. All four probes exhibited similar, bright one-photon-excited fluorescence emission ($\varepsilon(\Phi) = 1804–5148\,M^{-1}cm^{-1}$), indicating that they might serve as suitable imaging probes under physiological conditions.

We next assessed the inhibitory properties of these probes with recombinant human MAO-A and MAO-B by using the commercially available Amplex kit (Figure S3 and Figure 2 A); under identical assay conditions, all four probes were potent inhibitors of MAO-A and MAO-B, with IC_{50} values in the nanomolar range and some degree of preference towards MAO-B inhibition. Gratifyingly, **M2** showed a very good MAO-B/MAO-A selectivity score of 35.1, with IC_{50} values of 10.8 ± 1.2 nM and 379 ± 2.2 nM, respectively. For comparison, rasagiline (**RA**) showed a 105-fold selectivity over MAO-A. The inactivation kinetics were then studied to further show that **M2**, similar to **RA**, irreversibly inhibited MAO in a concentration- and time-dependent manner (Figure S3 C–F). None of the control probes showed significant

(A)

	MAO-A IC_{50}/nM	MAO-B IC_{50}/nM	MAO-B selectivity
M1	60.6 ± 0.2	24.5 ± 0.6	2.5
M2	379 ± 2.2	10.8 ± 1.2	35.1
M3	174 ± 0.5	40.0 ± 1.1	4.4
M4	59.1 ± 0.5	41.7 ± 0.8	1.4
RA	484 ± 5.0	4.61 ± 0.7	105

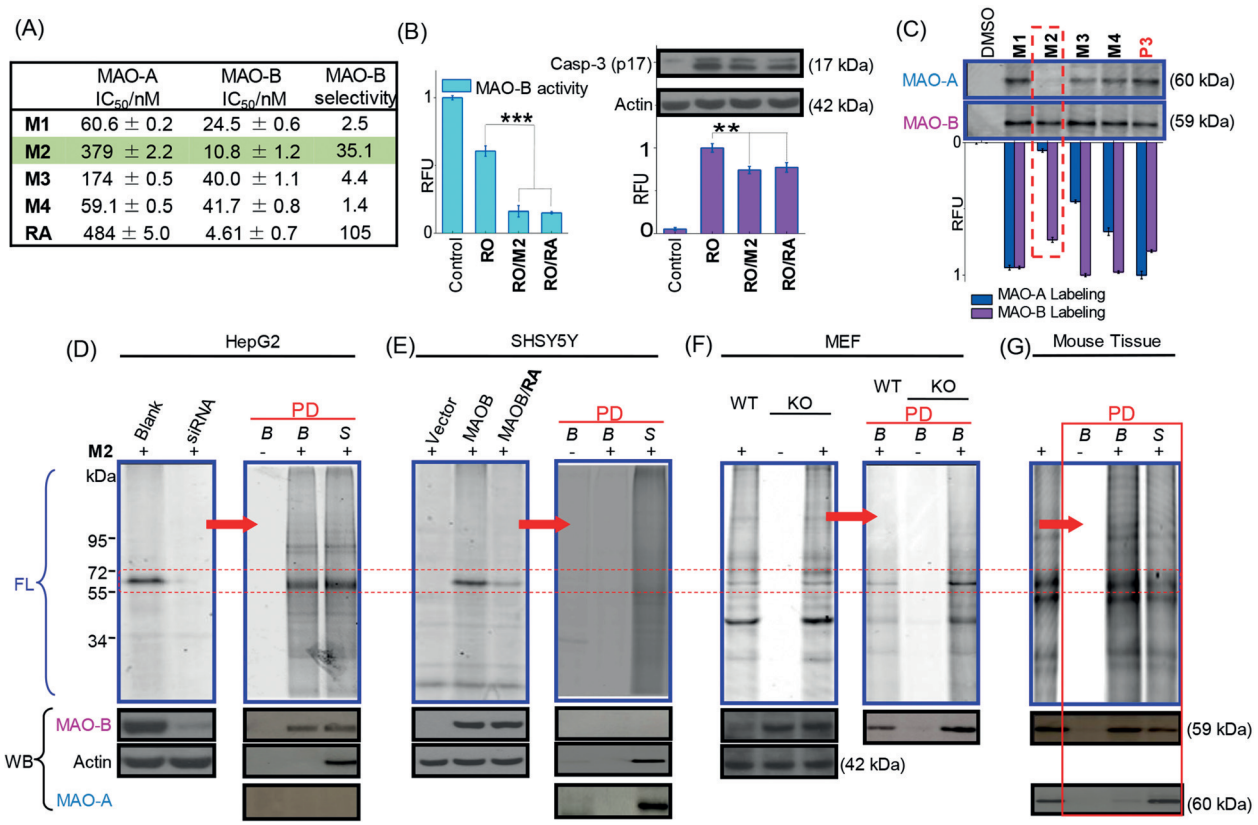

Figure 2. A) IC_{50} values of MAO-A and MAO-B inhibition with **M1**–**M4**. MAO-B selectivity = [IC_{50} of MAO-A]/[IC_{50} of MAO-B]. B) MAO-B activities (left) and cleaved caspase-3 (p17) expression levels (right: WB analysis; bottom: graphical representation) from **RO** induced HepG2 cells treated with **M2** or **RA**. ***$P < 0.001$, **$P < 0.01$, $n = 3$, student's t-test, two-tailed in (B). C) In-gel fluorescence scanning showing the labeling of human MAO-A and MAO-B by various probes (5 μM, 1 h). D) Proteome reactivity profiles of **M2** labeled HepG2 cells, before (left) and after affinity enrichment (right). Both blank and siRNA cells were labeled with **M2** (10 μM, 2 h; same in F/G). E) **M2** labeled SHSY5Y cells, either transfected with a Flag-MAO-B plasmid or vector control.[8] Left and right: before and after affinity enrichment. F) **M2** labeled wild-type (WT) or parkin-knockout (KO) MEFs. G) Mouse tissues labeled with **M2** (50 μM, 3 h), before and after enrichment. Affinity-enriched samples are shown in red boxes and are labeled (as PD). *B*: avidin bead-bound fraction, *S*: supernatant fraction. Bands of approximately 60 kDa are shown in red boxes (dotted line). FL: fluorescence gels (purple boxes). WB: Western blots (black boxes).

inhibition of the MAO activities (Figure S3), indicating the importance of the *N*-propargylamine group in the probe design. Rotenone (**RO**), a high-affinity inhibitor of complex I of the mitochondrial electron-transfer chain that is known to induce the generation of reactive oxygen species (ROS) and cause subsequent mitochondria-mediated apoptosis, was previously shown to cause the development of PD symptoms in cell-based models, presumably by the modulation of cellular MAO-B activities.[15] To investigate whether **M2** could ameliorate **RO** induced apoptosis through MAO-B inhibition, we pre-treated HepG2 (hepatocellular carcinoma) cells with **M2** (10 μM, 2 h) or **RA** (10 μM, 2 h), followed by treatment with **RO** (100 μM, 24 h; Figure 2B); a combination treatment of the cells with **RO** and **M2** (or **RA**) was found to cause significantly more down-regulation of the MAO-B activity, with a corresponding decrease in the activation of caspase-3 activity and apoptosis. We thus conclude that **M2**, similar to **RA**, is a potent cellular inhibitor of MAO-B.

We next investigated whether **M2** serves as an effective activity-based probe for the in situ proteome profiling of the endogenous MAO-B activity (Figure 2C–H). First, **M2**, together with other analogous probes (**M1**/**M3**/**M4**) and **P3**, was used to label recombinant MAO-A and MAO-B under identical conditions, and the corresponding probe-labeled adducts were analyzed by SDS-PAGE analysis and in-gel fluorescence scanning after a click reaction with Rh-biotin-N_3 (Figure 2C); whereas the use of **P3** led to nearly equal labeling of MAO-A and MAO-B, as previously reported,[9] **M2** was found to show an excellent preference for MAO-B labeling, as evidenced by the presence of a strongly fluorescent band (ca. 59 kDa) for the MAO-B reaction. On the contrary, the fluorescent band (ca. 60 kDa) of the **M2** labeled enzyme could be hardly detected when the same amount of MAO-A was labeled. Interestingly, two other probes, **M3** and **M4**, but not **M1**, also showed some degree of preference towards MAO-B labeling. These results are consistent with the inhibition data (Figure 2A). **M2** was thus chosen for all subsequent biological evaluations.

We first showed in a competitive experiment that MAO-B labeling by **M2** was completely abolished by the presence of an excess of **RA**, clearly indicating that it competed for binding to the same FAD-binding site in the enzyme (Figure S4). Dose-dependent labeling experiments indicated that as little as 50–100 nM of **M2** were sufficient to produce

a visible fluorescent band of labeled MAO-B. This detection sensitivity is comparable to that reported for **P3**.[9] To confirm the utility of **M2** for the selective profiling of MAO-B activities in a complex proteome, we next carried out cell-based proteome profiling in HepG2 and SHSY5Y cells (human-derived neuroblastoma), which are well-established disease cell lines possessing elevated levels of MAO-B (for HepG2) and MAO-A (for SHSY5Y) activity, respectively.[8,16] The corresponding knockdown (with MAO-B siRNA) and transfection (with a MAO-B expressing plasmid) experiments were carried out. As shown in Figure 2D, treatment of the MAO-B expressing live HepG2 cells with **M2** produced a highly MAO-B selective proteome reactivity profile showing a single 59 kDa fluorescent band, which was completely absent for siRNA-treated cells (left gels). Further PD/WB experiments (right gels), as well as PD/LC-MS/MS (Table S2), unequivocally confirmed that this band was that of endogenous MAO-B. Side-by-side comparison of **M2** and **P3** indicated that both probes labeled MAO-B equally effectively (Figure S4D). In MAO-A expressing SHSY5Y cells, however, **M2** was unable to label any endogenous MAO-A (Figure 2E; lane 1 in the left gel), but upon transient transfection of the cells with a MAO-B expressing plasmid, we detected a highly distinct, 59 kDa fluorescent band (lane 2), which was nearly eliminated in the presence of **RA** (lane 3). This band was attributed to MAO-B by both WB analysis of the transfected cells (Figure 2E, bottom gels) and subsequent PD/WB experiments on the enriched labeled proteomes (right gels). Results clearly indicate that with its extremely high selectivity towards MAO-B, **M2** did not label MAO-A in MAO-A expressing cells.

Encouraged by the above results, we next investigated potential applications of **M2** to evaluate the relationship between MAO-B expression and dopaminergic neuronal homeostasis in PD models.[8,17,18] The main pathology of PD is the loss of dopaminergic neurons near the substantia nigra pars compacta (SNpc) region of the midbrain, a region populated with strongly MAO-B expressing astrocytes.[2a,4] Parkin is a component in the ubiquitin proteasome system that mediates protein degradation.[18] Previously, the loss of the parkin function, which is associated with recessive parkinsonism, was reported to promote the expression of MAO-B, which is thought to contribute towards the pathogenicity in parkin-related PD cases.[18] To examine whether **M2** could report the inverse relationship between parkin and MAO-B expression, proteomes from mouse embryonic fibroblasts (MEFs) derived from parkin-knockout (KO) mice were labeled by **M2**, then detected by in-gel fluorescence scanning and WB analysis (Figure 2F; left); compared to wild-type (WT) MEFs, we observed elevated MAO-B expression in parkin-KO MEFs (see bottom WB gels in Figure 2F). The corresponding fluorescence gel (top) showed a weakly labeled band at approximately 59 kDa in both WT and parkin-KO MEFs, with a slight increase in the labeling intensity of the latter. These signals were readily boosted by a simple affinity enrichment of the labeled proteomes (Figure 2F; right); upon PD, we observed an obvious intensity increase for the 59 kDa fluorescent band in the parkin-KO proteome, and again, this band was unequivocally assigned to the elevated endogenous MAO-B activities by WB analysis (bottom). Finally, the freshly prepared brain of a 24-month-old C57/B6 mouse that expressed both MAO-A and MAO-B, as confirmed by WB analysis (Figure 2G, bottom), was labeled with **M2** and analyzed as is (Figure 2G, left lane) or after affinity enrichment (red boxes); we again observed a fluorescently labeled band corresponding to endogenous MAO-B, but none that are due to MAO-A (verified by PD/WB in Figure 2G, bottom gels). The higher background fluorescence labeling in the gel was likely caused by the intrinsically complicated process of mouse tissue preparation. Large-scale PD/LC-MS/MS experiments were used to identify the other labeled proteins in the MEFs (ca. 40 kDa band in Figure 2F) and mouse tissues (ca. 55 kDa band in Figure 2G), and the results are summarized in Tables S3 and S4. Further validation will be needed to confirm whether these putative "hits" were genuine "off targets" of **M2**. Notwithstanding, the fact that only few proteins were positively identified from such experiments already indicates the extremely high selectivity of **M2** towards endogenous MAO-B.

Finally, the live-cell MAO-B imaging capability of **M2** was investigated by confocal microscopy. **M2** was added to a medium containing growing HepG2 cells. Upon incubation and subsequent replacement with **M2** free media, the cells were directly imaged under the probe channel ($\lambda_{ex} = 405$ nm). Immunofluorescence (IF) experiments with anti-MAO-B antibodies were performed on the same cells. As shown in Figure 3, **M2** treated cells showed strong fluorescence signals

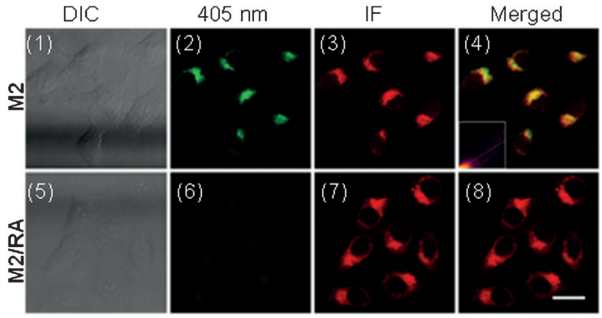

Figure 3. Images of HepG2 cells with **M2** (2 μM, 2 h) with or without **RA** (10×, 1 h pretreatment). Panels 1 and 5: differential interference contrast (DIC) images; panels 2 and 6: one-photon images ($\lambda_{ex} = 405$ nm); panels 3 and 7: IF panels with anti-MAO-B antibody; panels 4 and 8: merged images of panels 2/3 and 6/7. Inset: colocalization analysis of 2/3, giving $R = 0.78$. Scale bar: 25 μm.

(panel 2) that mostly overlapped with those from the IF panel (panel 3; $R = 0.78$); these signals were completely abolished in cells pretreated with **RA**, indicating that they were due to MAO-B bound **M2**. No fluorescence signal was detected in **NP2** treated HepG2 cells or **M2** treated SHSY5Y cells (Figure S5), reaffirming the high MAO-B selectivity of **M2** in imaging applications. Unlike **U1**, whose live-cell imaging fluorescence signals were readily washed away,[8] signals from **M2** treated cells persisted after prolonged washes (data not shown), indicating that **M2** had been covalently attached to endogenous MAO-B, and should provide higher spatial resolution in future bioimaging experiments.

In conclusion, we have successfully developed the first small-molecule probe that is capable of both in situ proteome profiling and live-cell bioimaging of MAO-B activities from a variety of biological samples, including well-established cell and tissue models of Parkinson's disease. Our probe provides diffusion-free live-cell/tissue imaging and enables the sensitive detection of endogenous MAO-B activities from complex proteome samples in an isoform-selective manner.

Acknowledgements

Funding was provided by the Faculty of Science, NUS (R-143-000-521-112) and the National Medical Research Council (NMRC/1260/2010, NMRC/BNIG/2011/2013, and CBRG/0038/2013) of Singapore. We also acknowledge the generous donation of the probe **P3** by Rolf Breinbauer (TU Graz).

Keywords: activity-based probes · imaging · monoamine oxidases · Parkinson's disease · proteomics

How to cite: *Angew. Chem. Int. Ed.* **2015**, *54*, 10821 – 10825
Angew. Chem. **2015**, *127*, 10971 – 10975

[1] J. C. Shih, K. Chen, M. J. Ridd, *Annu. Rev. Neurosci.* **1999**, *22*, 197 – 217.
[2] a) M. B. H. Youdim, D. Edmondson, K. F. Tipton, *Nat. Rev. Neurosci.* **2006**, *7*, 295 – 309; b) M. Bortolato, K. Chen, J. C. Shih, *Adv. Drug Delivery Rev.* **2008**, *60*, 1527 – 1533; c) J. P. Finberg, M. B. Youdim, *Neuropharmacology* **1983**, *22*, 441 – 446.
[3] a) A. M. Gorman, A. McGowan, C. O'Neill, T. Cotter, *J. Neurol. Sci.* **1996**, *139*, 45 – 52; b) M. P. Mattson, *Nat. Rev. Mol. Cell Biol.* **2000**, *1*, 120 – 129.
[4] a) A. Nicotra, F. Pierucci, H. Parvez, O. Senatori, *Neurotoxicology* **2004**, *25*, 155 – 165; b) P. Damier, A. Kastner, Y. Agid, E. C. Hirsch, *Neurology* **1996**, *46*, 1262 – 1269.
[5] a) N. J. Ives, R. L. Stowe, J. Marro, C. Counsell, A. Macleod, C. E. Clarke, R. Gray, K. Wheatley, *Br. Med. J.* **2004**, *329*, 593; b) R. E. Heikkila, L. Manzino, F. C. Cabbat, R. C. Duvoisin, *Nature* **1984**, *311*, 467 – 469; c) M. B. H. Youdim, A. Gross, J. P. M. Finberg, *Br. J. Pharmacol.* **2001**, *132*, 500 – 506.
[6] a) G. Chen, D. J. Yee, N. G. Gubernator, D. Sames, *J. Am. Chem. Soc.* **2005**, *127*, 4544 – 4545; b) E. A. Albers, K. A. Rawls, C. J. Chang, *Chem. Commun.* **2007**, 4647 – 4649; c) J. X. Aw, Q. Shao, Y. Yang, T. Jiang, C. Ang, B. Xing, *Chem. Asian J.* **2010**, *5*, 1317 – 1321; d) D. Kim, S. Sambasivan, H. Nam, K. H. Kim, J. Y. Kim, T. Joo, K.-H. Lee, K.-T. Kim, K. H. Ahn, *Chem. Commun.* **2012**, *48*, 6833 – 6835.
[7] a) S. B. Long, L. Chen, Y. Xiang, M. Song, Y. Zheng, Q. Zhu, *Chem. Commun.* **2012**, *48*, 7164 – 7166; b) X. Li, J. Yu, Q. Zhu, L. Qian, L. Li, Y. Zheng, S. Q. Yao, *Analyst* **2014**, *139*, 6092 – 6095.
[8] L. Li, C. Zhang, G. Y. J. Chen, B. Zhu, C. Chai, Q.-H. Xu, E.-K. Tan, Q. Zhu, K.-L. Lim, S. Q. Yao, *Nat. Commun.* **2014**, *5*, 3276.
[9] J. M. Krysiak, J. Kreuzer, P. Macheroux, A. Hermetter, S. A. Sieber, R. Breinbauer, *Angew. Chem. Int. Ed.* **2012**, *51*, 7035 – 7040; *Angew. Chem.* **2012**, *124*, 7142 – 7147.
[10] A. K. Upadhyay, D. E. Edmondson, *Biochemistry* **2009**, *48*, 3928 – 3935.
[11] B. F. Cravatt, A. T. Wright, J. W. Kozarich, *Annu. Rev. Biochem.* **2008**, *77*, 383 – 414.
[12] Y. Su, S. Pan, Z. Li, L. Li, X. Wu, P. Hao, S. K. Sze, S. Q. Yao, *Sci. Rep.* **2015**, *5*, 7724.
[13] a) L. E. Edgington, A. B. Berger, G. Blum, V. E. Albrow, M. G. Paulick, N. Lineberry, M. Bogyo, *Nat. Med.* **2009**, *15*, 967 – 973; b) Z. Li, D. Wang, L. Li, S. Pan, Z. Na, C. Y. J. Tan, S. Q. Yao, *J. Am. Chem. Soc.* **2014**, *136*, 9990 – 9998.
[14] Y. Su, J. Ge, B. Zhu, Y.-G. Zheng, Q. Zhu, S. Q. Yao, *Curr. Opin. Chem. Biol.* **2013**, *17*, 768 – 775.
[15] P. Caboni, T. Sherer, N. Zhang, G. Taylor, H. Na, J. Greenamyre, J. Casida, *Chem. Res. Toxicol.* **2004**, *17*, 1540 – 1548.
[16] a) J. C. Shih, K. Chen, *Curr. Med. Chem.* **2004**, *11*, 1995 – 2005; b) M. Naoi, W. Maruyama, Y. Akao, H. Yi, Y. Yamaoka, *J. Neural Transm. Suppl.* **2006**, *71*, 67 – 77.
[17] B. E. Riley et al., *Nat. Commun.* **2013**, *4*, 1982.
[18] H. Jiang, Q. Jiang, W. Liu, J. Feng, *J. Biol. Chem.* **2006**, *281*, 8591 – 8599.

Received: May 15, 2015
Revised: July 3, 2015
Published online: July 21, 2015

